ARMY RESEARCH LABORATORY

Signal Processing Technique to Remove Signature Distortion in ARL Synchronous Impulse Reconstruction (SIRE) Ultra-Wideband (UWB) Radar

by Lam Nguyen

NOTICES

Disclaimers

The findings in this report are not to be construed as an official Department of the Army position unless so designated by other authorized documents.

Citation of manufacturer's or trade names does not constitute an official endorsement or approval of the use thereof.

Destroy this report when it is no longer needed.   Do not return it to the originator.

Army Research Laboratory

Adelphi, MD 20783-1197

ARL-TR-4404   **March 2008**

Signal Processing Technique to Remove Signature Distortion in ARL Synchronous Impulse Reconstruction (SIRE) Ultra-Wideband (UWB) Radar

Lam Nguyen
Sensors and Electron Devices Directorate, ARL

REPORT DOCUMENTATION PAGE

1. REPORT DATE *(DD-MM-YYYY)*	2. REPORT TYPE	3. DATES COVERED *(From - To)*
March 2008	Ongoing Research	

4. TITLE AND SUBTITLE	5a. CONTRACT NUMBER
Signal Processing Technique to Remove Signature Distortion in ARL Synchronous Impulse Reconstruction (SIRE) Ultra-Wideband (UWB) Radar	5b. GRANT NUMBER
	5c. PROGRAM ELEMENT NUMBER

6. AUTHOR(S)	5d. PROJECT NUMBER
Lam Nguyen	5e. TASK NUMBER
	5f. WORK UNIT NUMBER

7. PERFORMING ORGANIZATION NAME(S) AND ADDRESS(ES)	8. PERFORMING ORGANIZATION REPORT NUMBER
U.S. Army Research Laboratory ATTN: AMSRD ARL SE RU 2800 Powder Mill Road Adelphi, MD 20783-1197	ARL-TR-4404

9. SPONSORING/MONITORING AGENCY NAME(S) AND ADDRESS(ES)	10. SPONSOR/MONITOR'S ACRONYM(S)
	11. SPONSOR/MONITOR'S REPORT NUMBER(S)

12. DISTRIBUTION/AVAILABILITY STATEMENT

Approved for public release; distribution unlimited.

13. SUPPLEMENTARY NOTES

14. ABSTRACT

ARL has designed and developed the SIRE UWB SAR radar in support of the U.S. Army vision for increased mobility, survivability, and lethality. The radar is based on time-domain wideband impulses. For this radar, ARL designed and implemented a data acquisition technique called Synchronous Impulse Reconstruction (SIRE) that allowed us to employ relatively slow ADC (40 MHz) to digitize wideband signals (>3000 MHz). However, the scheme assumed that the radar and targets are stationary during the data acquisition cycle and in reality the target signatures did suffer the distortions in phase and shape due to the radar motion. The phase error would lead to significant loss in target radar cross section values in resulting SAR imagery. The shape errors would destroy the frequency contents of the targets and thus the ability to discriminate targets from other confuser classes.

This report describes a signal processing technique that removes the phase and shape distortions in the radar signal due to the motion of the platform. This technique results in SAR imagery with significant improvement in focus quality and signal-to-noise level. This has been tested and verified with simulated and measured radar data. This technique could be applied for any time-based impulse radar system that experiences the relative motion between the radar and the targets during the data acquisition cycle.

15. SUBJECT TERMS

Ultra wideband radar, synthetic aperture radar (SAR), Forward imaging radar

16. SECURITY CLASSIFICATION OF:			17. LIMITATION OF ABSTRACT	18. NUMBER OF PAGES	19a. NAME OF RESPONSIBLE PERSON
a. REPORT	b. ABSTRACT	c. THIS PAGE	SAR	22	Lam Nguyen
U	U	U			19b. TELEPHONE NUMBER *(Include area code)* 301-394-0847

ii

Contents

List of Figures

List of Tables

1. Introduction

In support of the U.S. Army vision for increased mobility, survivability, and lethality, the U.S. Army Research Laboratory (ARL) has recently developed the forward-looking ultra-wideband (UWB) synthetic aperture radar (SAR) (*1, 2, 3*). The radar transmits and receives short impulses that cover the frequency spectrum from 300 MHz to 3000 MHz. Conventionally, very high speed analog-to-digital converters (ADCs) are required to directly digitize these time domain impulses. Although this conventional technique allows the radar design to be simple, it is too costly to build the high speed ADCs that can directly digitize the wide-bandwidth returned impulses. Therefore, ARL has developed a sampling technique that allows us to employ inexpensive ADCs to digitize wide bandwidth signals. This technique is called Synchronous Impulse REconstruction (SIRE). This is a modified and enhanced version of the equivalent time-sampling technique that is widely used in commercial digital storage oscilloscopes (*4*) and some radar (*5*). As mentioned, the advantage of this technique (or other equivalent time-sampling techniques) is that it relieves the speed requirements for the ADCs. However, the data acquisition time for signal reconstruction increases. If the radar is stationary during this data acquisition cycle, the radar signal will be perfectly reconstructed from the returned impulses. However, this assumption is not true since the relative position between the radar and the targets is no longer negligible during the data acquisition cycle because of the motion of the radar platform. This is especially true for forward-looking radar since the radar moves toward the imaging area. This relative motion between the radar and the targets during the data acquisition cycle results in severe phase and shape distortions in the reconstructed signal. This in turn results in poor focus quality and low signal-to-noise level in SAR imagery.

This report describes a signal-processing technique that removes the phase and shape distortions from the radar signal, which are attributable to the motion of the platform. This technique results in SAR imagery with significant improvement in focus quality and signal-to-noise level. This has been tested and verified with simulated and measured radar data. This technique could be applied for any time-based impulse radar system that experiences the relative motion between the radar and the targets during the data acquisition cycle.

2. Signal-Processing Technique to Compensate for Forward Motion

2.1   The ARL SIRE Technique

The ARL SIRE radar system (*3*) employs an Analog Devices 12-bit 80-MHz ADC to digitized returned radar signals. However, the ADC is clocked at the system clock rate of 40 MHz. From the basic sampling theory (*4*), it is not possible to reconstruct the wide-bandwidth signal (300

MHz to 3000 MHz) since this ADC rate is much slower than the required minimum Nyquist[1] sampling rate (6000 MHz). However, by using the synchronous time equivalence sampling technique, we can achieve a much higher equivalent sampling rate. Figure 1 provides a graphical representation of the SIRE data acquisition technique.
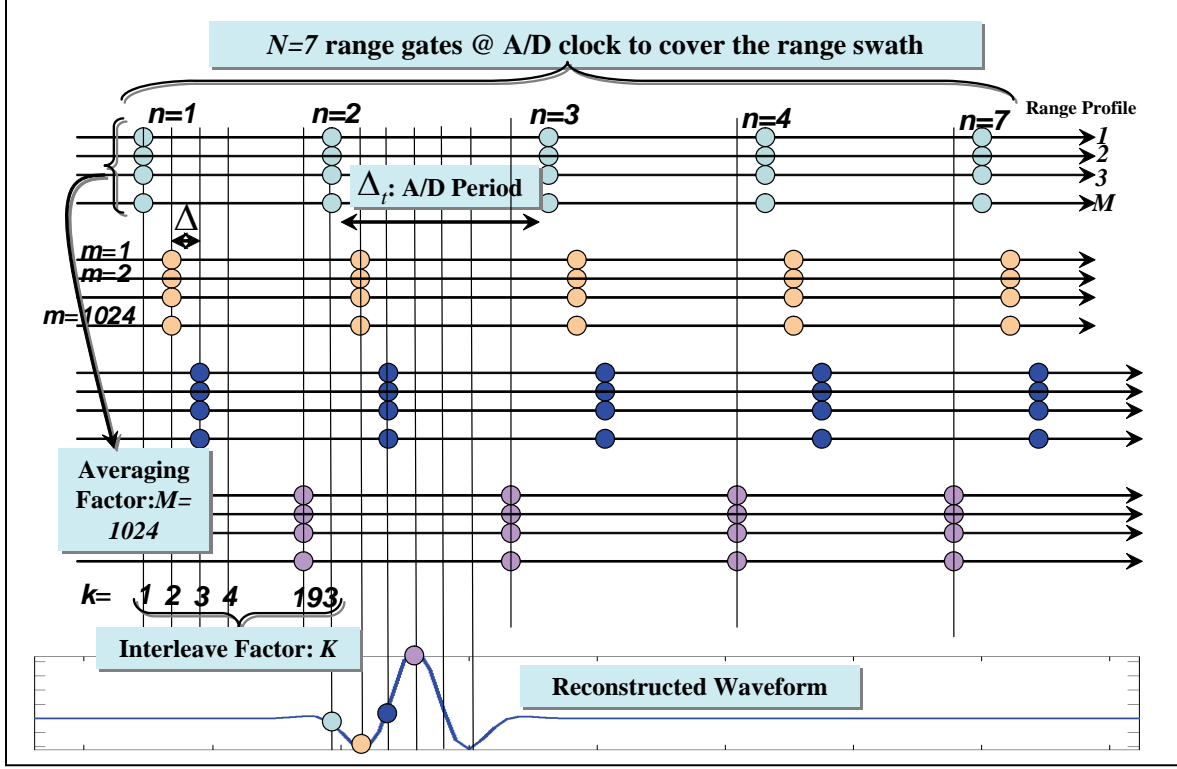
Figure 1. The ARL synchronous impulse reconstruction data acquisition scheme. (This is a modified and enhanced version of the equivalent time-sampling technique.)

The ADC sampling period is Δ_t; the value of this parameter in figure 1 is 25 nsec, which corresponds to an analog-to-digital (A/D) sampling rate of 40 MHz. The number of samples for each range profile is denoted by N, which is equal to 7 in our example. This corresponds to a range swath of 30 m. The system pulse repetition frequency (*PRF*) is 1 MHz. The system pulse repetition interval ($PRI = \dfrac{1}{PRF}$), i.e., the inverse of *PRF*, is 1 micro-second ((mu)s). Each aliased (slowly sampled at A/D speed) radar record is measured M times (1024 in this example) and the records are integrated to achieve a higher signal-to-noise level. After M repeated measurements of the same range profile are summed, the first range (fast-time) bin is increased by Δ. Thus, the next group of M range profiles is digitized with a timing offset of Δ with respect to the transmit pulse. The parameter Δ represents a time sample spacing that satisfies the Nyquist criterion for the transmitted radar signal. For the cited case in figure 1, this time sample spacing is 129.53 pico-seconds, which corresponds to a sampling rate of 7.72 GHz. This

---

[1]Nyquist is the person who invented this theory.

effective sampling rate is sufficient for the wide-bandwidth radar signal (300 MHz to 3000 MHz). Note that the number of interleaved samples is

$$K = \frac{\Delta_t}{\Delta},$$

(1)

which is 193 in figure 1. After *K* groups of *M* pulses are transmitted and the return signals are digitized and summed by the Xilinx Spartan[2] 3 field programmable gate-array (FPGA), this results in a radar record of *N.K* samples with an equivalent of fast sample spacing of Δ. The total time to complete one data acquisition cycle is *N.K.PRI*, which is 197.6 msec in this case. Please note that during the entire data acquisition cycle period (197.6 msec), the relative position between the radar and the targets is assumed to be stationary. Table 1 summarizes the parameters used by the SIRE data acquisition technique.

Table 1. Summary of radar parameters.

Radar pulse repetition frequency (*PRF*)	1 MHz
Radar pulse repetition interval (*PRI*)	1e-6 sec
ADC sampling rate	40 MHz
ADC sampling period	25 nsec
Number of ADC (slow) range gates (*N*)	7
Interleaving factor (*K*)	193
Number of repeated measurements for averaging (*M*)	1024
Total number of range gates (*N.K)*	1351
Effective sampling period (time-equivalent)	129.53e-12 sec
Effective sampling rate (time-equivalent)	7.72 GHz
Total data acquisition time	197.6 msec

2.2 Perfect Reconstruction of the Radar Signal With Stationary Radar Platform

Let us consider the first simulation case. The radar is situated 10 m away from a point target. The radar transmits impulse signals to the point target. The receiver performs the data acquisition on returned signals using the sampling technique described in previous section. After *M.K* (1024x193) pulses are transmitted and received, the data acquisition cycle is completed and the radar waveform is reconstructed. In this case, since the radar is stationary, the reconstructed waveform is perfect. Figure 2 shows both the time domain and frequency domain of the reconstructed waveform with stationary radar.

[2]Xilinx Spartan is a registered trademark of Xilinx, Inc.
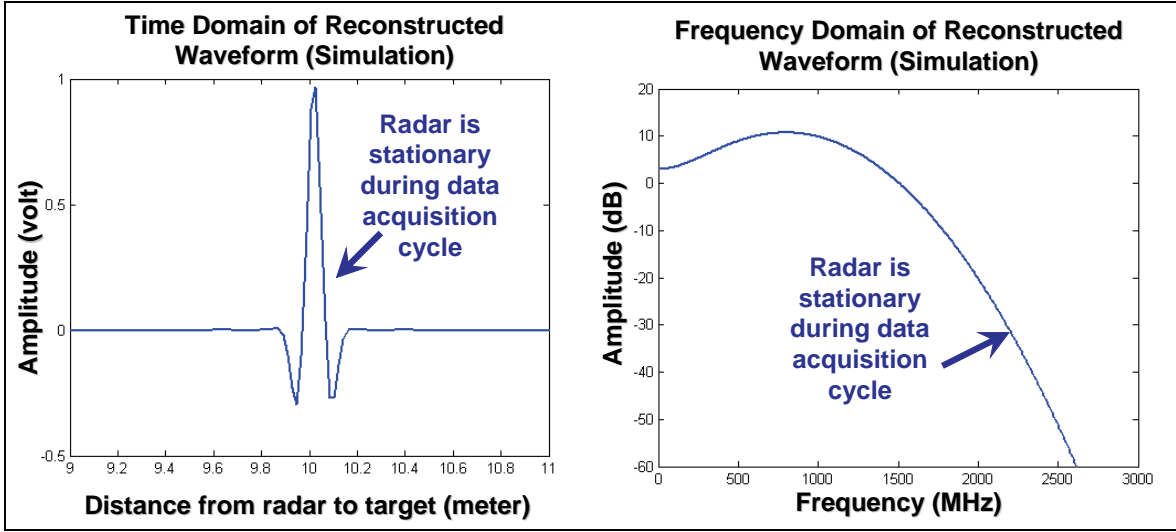
Figure 2. Perfect reconstruction with stationary radar.

2.3   Phase and Amplitude Distortions in Reconstructed Radar Signals With Moving Platform

Next, we want to illustrate the problem when the radar is moving during the data acquisition cycle. This is the same simulation case as in previous section except that the radar is moving toward the target at the speed of 5 miles per hour. In figure 3, we show the reconstructed waveform of the moving case versus the stationary case. In the time domain plot of figure 3, we can notice a significant phase shift in the reconstructed waveform compared with the ideal case (stationary). The phase information is crucial for the SAR image formation process since radar signals are coherently processed by the image former. In addition to the phase shift, the frequency domain plot of the moving case (figure 3) indicates that there is a distortion in the shape of the reconstructed waveform. The amount of phase shift and shape distortions changes as the distance from the radar to the target varies. Figure 4 shows the reconstruction waveform of another simulation case that is similar to the case in figure 3, except that the distance between the radar and the target is 15 m instead of 10 m. In addition to the distance between the radar and the target, the speed of the platform contributes to the amount of distortions. Figure 5 shows the reconstructed waveform similar to the simulation case in figure 4, except that the radar platform's speed is increased to 12 miles per hour.

4
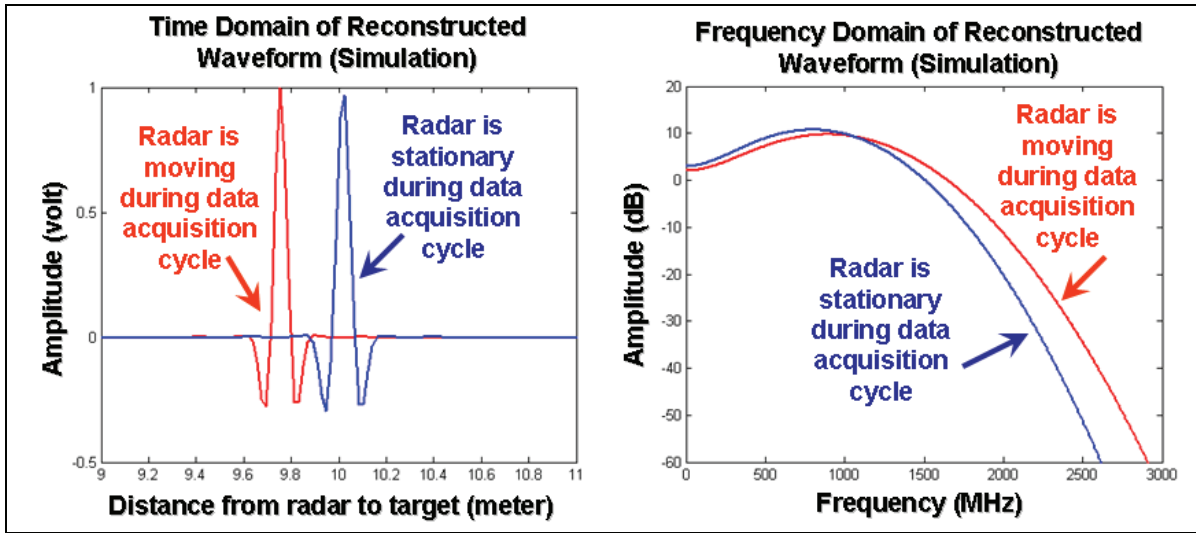
Figure 3. Phase and shape distortions in reconstructed waveform (red). (The distance between the radar and the target is 10 m. The speed of the radar platform is 5 miles per hour. The ideal reconstructed waveform [stationary radar] is shown in blue.)
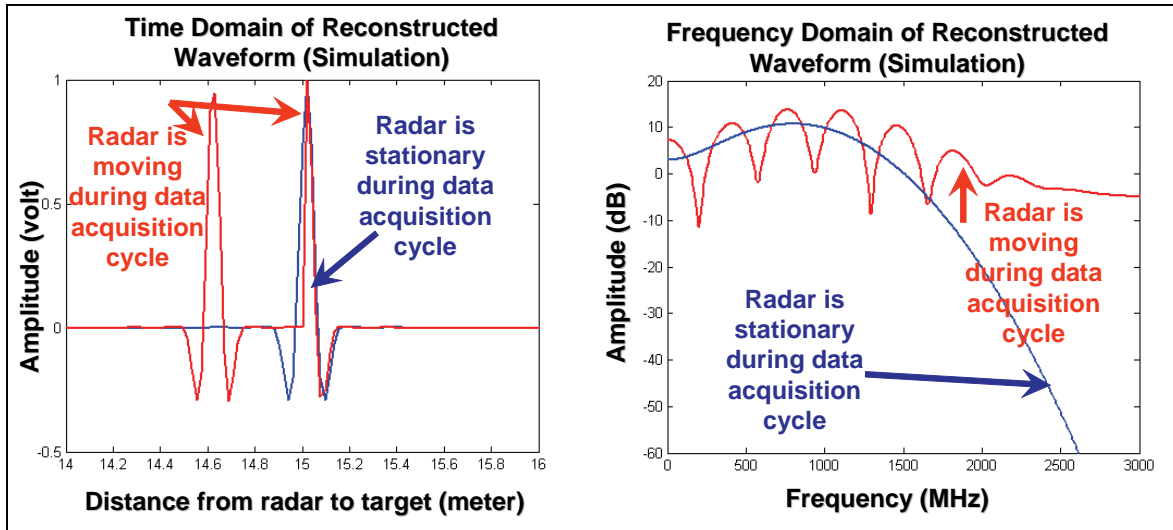
Figure 4. Phase and shape distortions in reconstructed waveform (red). (The distance between the radar and the target is 15 m. The speed of the radar platform is 5 miles per hour. The ideal reconstructed waveform [stationary radar] is shown in blue.)
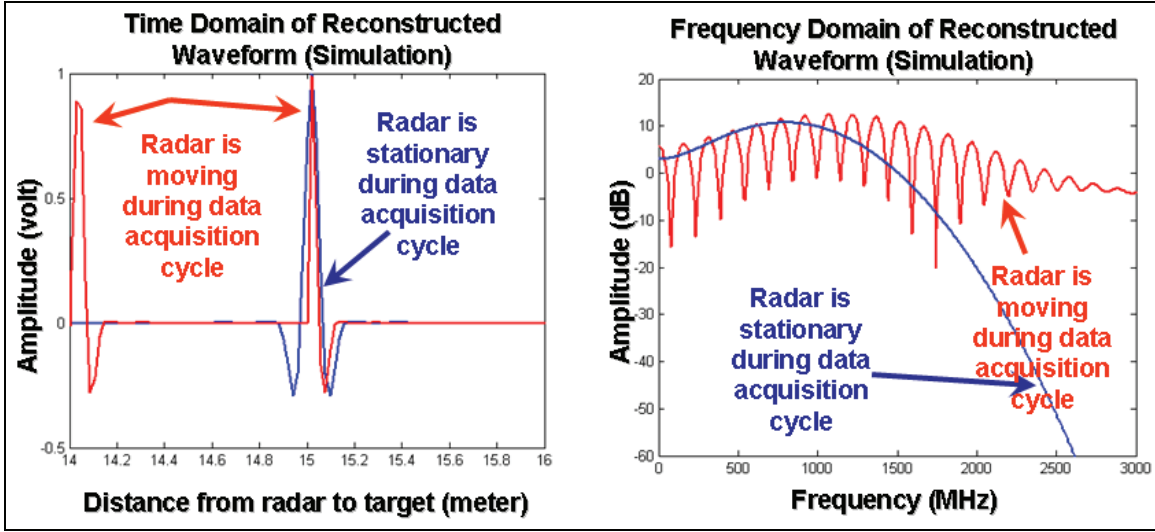
Figure 5. Phase and shape distortions in reconstructed waveform (red). (The distance between the radar and the target is 15 m. The speed of the radar platform is 12 miles per hour. The ideal reconstructed waveform [stationary radar] is shown in blue.)

2.4 Technique to Remove the Phase and Shape Distortions From Reconstructed Waveforms

In this section, we discuss the technique to remove the phase and shape distortions from the reconstructed waveforms. We show the results using simulated data and real radar data.

The phase and shape distortions in the reconstructed waveform can be explained as follow. Figure 6 shows the data acquisition scheme when the radar is moving during the data acquisition cycle. For the reconstructed waveform, the effective sampling period is Δ_m, which no longer has the same value as Δ in figure 1. After transmitting and receiving the first M pulses, the radar starts the second group of M pulses with the timing offset of Δ from the previous group. During the data acquisition time for the first M pulses, in this case, the radar has traveled a distance of

$$d = v.M.PRI \tag{2}$$

in which v is the speed of the radar during this acquisition group of M pulses, and PRI is the pulse repetition rate mentioned in section 2.1.

6
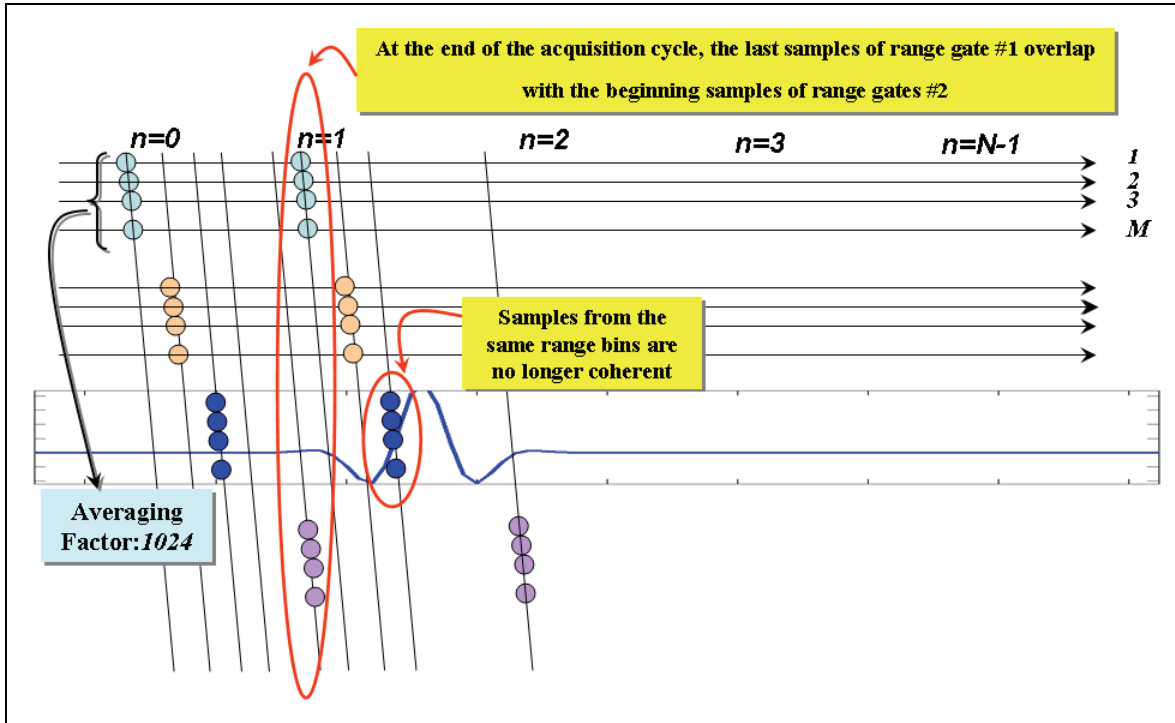
Figure 6. The ARL synchronous impulse reconstruction data acquisition scheme when the radar is moving during the data acquisition cycle.

The distance d corresponds to the elapsed time of

$$t = \frac{2d}{c}$$

$$= \frac{2v.M.PRI}{c} \tag{3}$$

in which $c = 3 \times 10^8$ is the speed of light.

Thus, the effective sampling period for the reconstructed waveform is

$$\Delta_m = \Delta + t$$

$$= \Delta + \frac{2v.M.PRI}{c} \tag{4}$$

From equation 4, the effective sampling period for the reconstructed waveform is varied with the radar's instantaneous speed. This generates the phase and shape distortion in the reconstructed waveform. Another source of artifact in the reconstructed waveform is depicted in figure 6. The last samples of the first range (measured at the slower A/D rate) overlap with the beginning samples of the second range gate. This creates the spurious glitches in the reconstructed waveforms (shown in figures 4 and 5). From equations 2 to 4, we assume that the radar speed v

7

is constant during the entire data acquisition cycle. This is not a bad assumption since the radar is moving slowly and its speed should not change too much during the period of 197 msec.

Let s_m be the reconstructed waveform with phase and shape distortions attributable to the radar platform's motion during the data acquisition cycle. Given the average speed of the radar platform at the time the measurement is made, we want to compute the ideal reconstruction s from the distorted s_m as if the radar is stationary during the data acquisition cycle. The system employs a differential global positioning system (GPS) system to measure the radar locations along the path. In addition, the GPS time stamps are recorded with the radar data stream. With the radar coordinates and time stamps information from two successive locations, the average speed of the radar at every location can be computed. The procedure to compensate for the phase and shape distortions in the radar signatures is as follows.

First, the distorted radar signal s_m is measured.

Next, the avarage speed at this position is computed as

$$v = \frac{\sqrt{(x_i - x_{i-1})^2 + (y_i - y_{i-1})^2 + (z_i - z_{i-1})^2}}{t_i - t_{i-1}} \tag{5}$$

in which $(x_{i-1}, y_{i-1}, z_{i-1})$ are the coordinates of the radar at the previous acquisition cycle (t_{i-1}), and (x_i, y_i, z_i) are the coordinates of the radar at the current acquisition cycle (t_i).

The equivalent sampling period for this acquisition cycle Δ_m is then computed as specified by equation 4. The distorted radar signal $s_m(n)$ is divided into N sub-signals as

$$s_{mi} = s_m(l), \qquad \text{where} \, 1 + (i-1)K \leq l \leq iK \text{ and} 1 \leq i \leq N . \tag{6}$$

Each sub-signal s_{mi} is then re-sampled with the use of the computed sampling period Δ_m

$$s_i = P(s_{mi}, \Delta_m, \Delta) \tag{7}$$

in which P is the interpolation process that re-samples the signal from the sampling period Δ_m to the new sampling period Δ_m.

The reconstructed waveform is the concatenation of N sub-signals

$$s = [s_0, s_1, ..., s_i, ..., s_N] \tag{8}$$

2.5   Results

2.5.1 Results Using Simulated Data

We applied the technique described in section 2.4 to the distorted signature (red in figure 4). The time and frequency results are plotted in figure 7. The distorted signature is perfectly reconstructed. The shape distortion is removed and its phase is aligned with the original stationary signature.

8
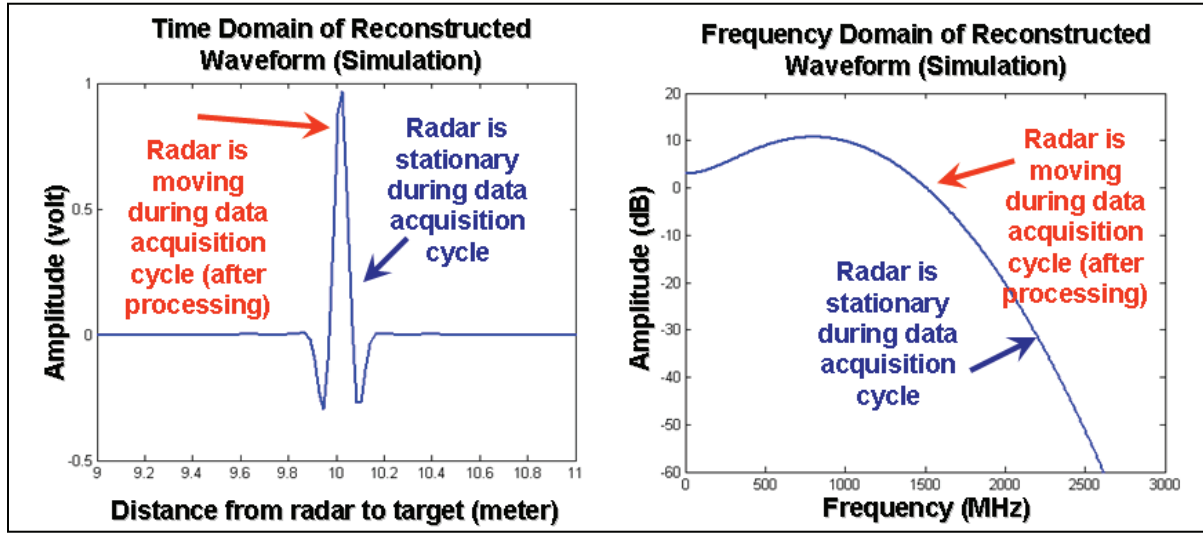
Figure 7. The technique is applied to the simulated data (in figure 4). (This figure shows the perfect reconstruction with the processing technique.)

2.5.2 Results Using Measured Radar Data

The ARL SIRE radar system has an array of 16 receivers that form a 2-m aperture and two transmitters that are situated at the ends and above the receiving array. The radar transmits *M* impulses using the left transmitter and simultaneously digitizes and integrates the return radar signals from 16 receiving channels. The radar then switches to the right transmitter and repeats the same process. The integration is performed by the FPGA in the radar hardware. Each time a transmitter is selected, the radar generates one data frame that includes data from all 16 receivers. Figure 8 shows seven frames of radar signatures from an 8-foot trihedral as the radar moves toward the target at the speed of 5 mph. In each data frame, we should expect two responses: a) the first large response from the trihedral, and b) a much weaker response because of the transmitter artifact. However, we can notice the obvious shape distortion that occurred in frames 1, 2, 4, and 6. In frames 2 and 6, the main responses split while in frames 1 and 4, the secondary responses split. In addition to the shape distortion, the phase errors are present. We applied the technique described in section 2.4 to these data. Figure 9 shows the data after processing. Notice that the phase and shape distortions of the trihedral signatures are corrected in figure 9. Figure 10 shows the time domain response of the same trihedral before and after forward motion processing.

9
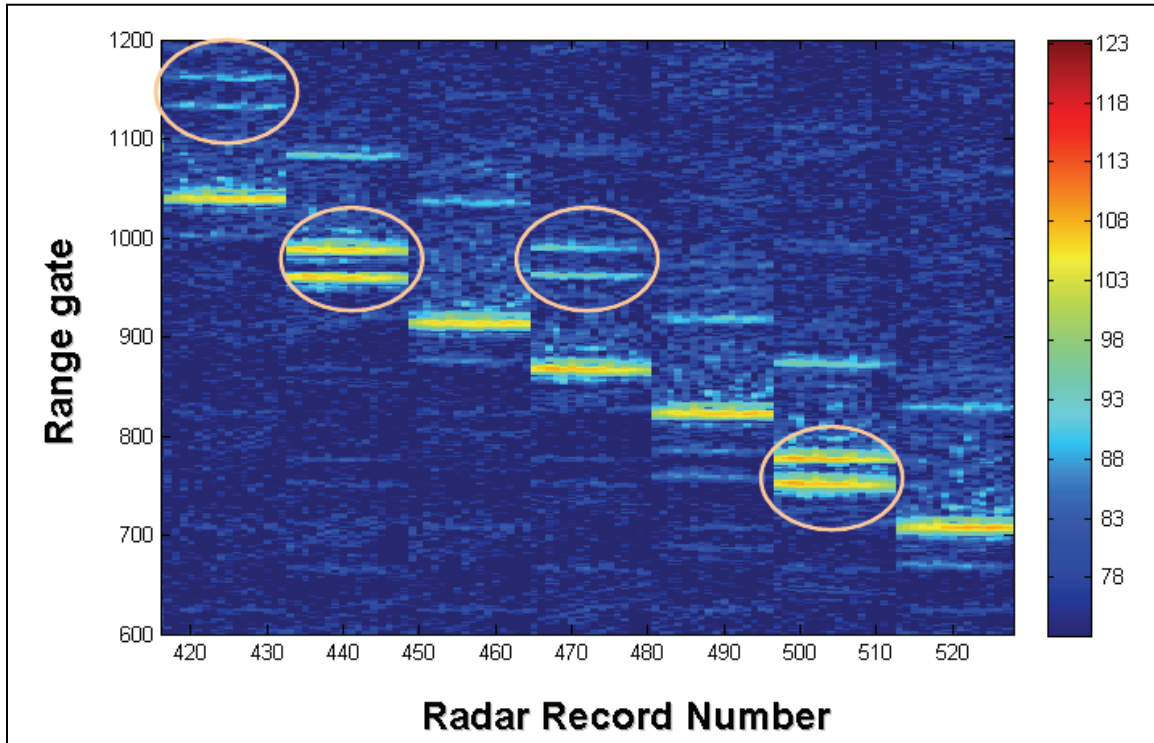
Figure 8. Raw radar data measured by ARL SIRE. (The radar moves at 5 mph toward an 8-ft trihedral. This figure shows the distortions in radar signatures when the radar is moving during the data acquisition cycle.)
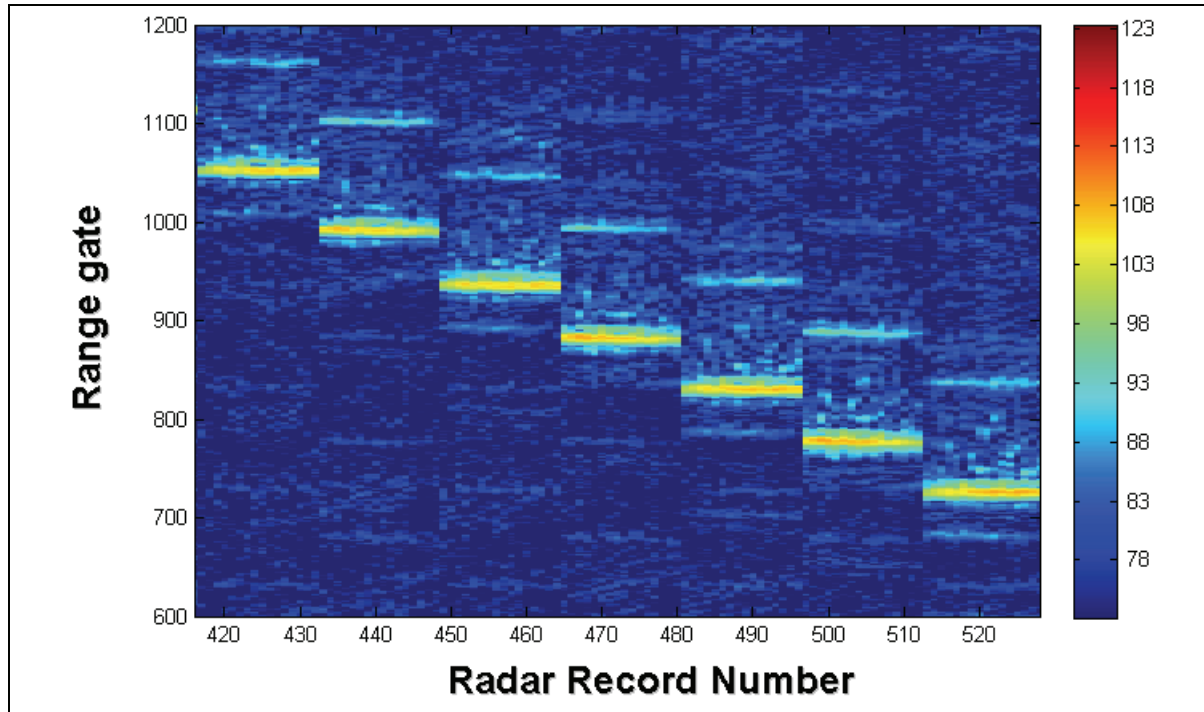
Figure 9. Data in figure 8 have been processed with the described processing technique. (The distortions in radar signatures have been removed.)
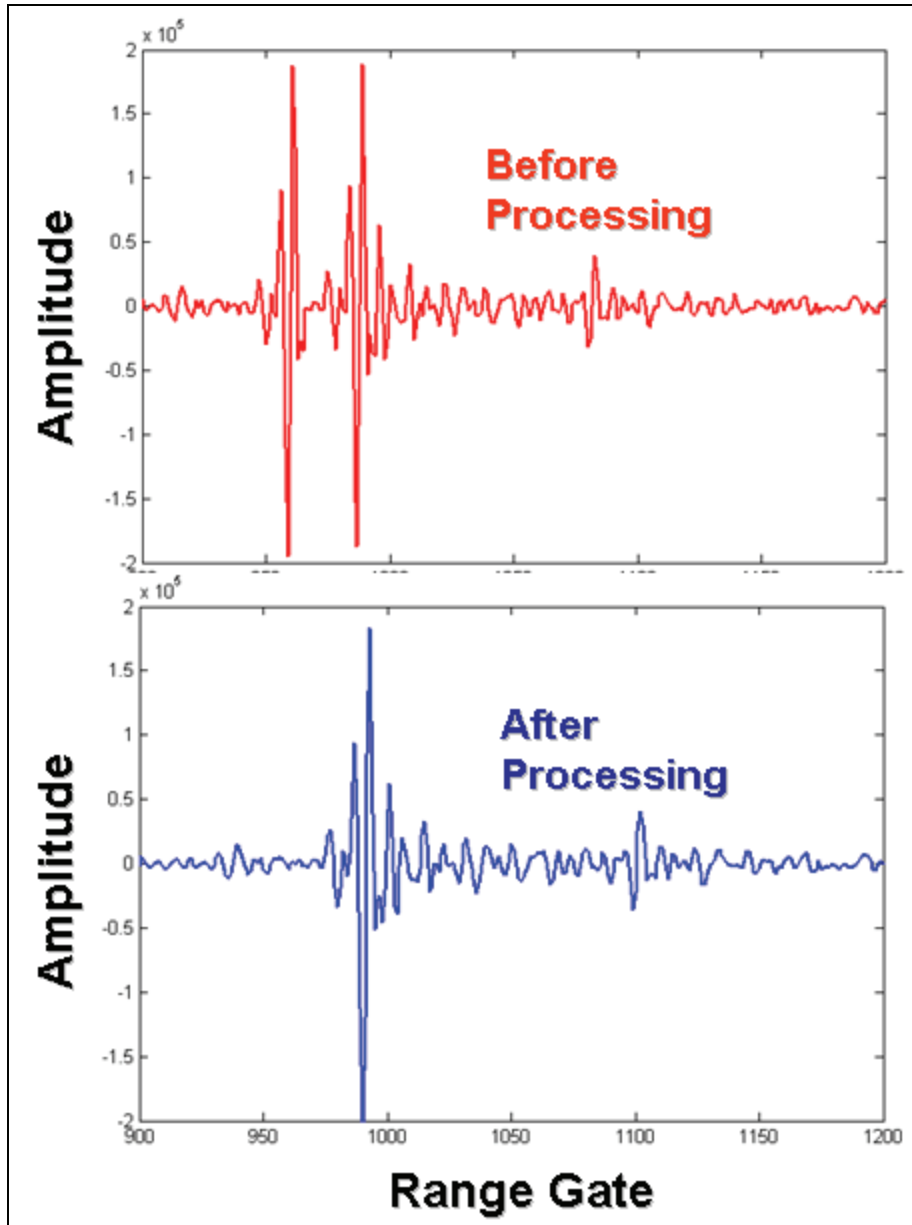
Figure 10. A down-range profile through a trihedral before and after processing.

We have seen the effect of radar forward motion on the radar signature. After all the signal-processing algorithms are performed on radar phase history data, the back-projection image formation algorithm is applied to the radar data to produce a SAR image.

Over the last decade, ARL has been using the back-projection image formation for various applications (*8 through 11*). In this forward imaging case, the back-projection algorithm uses a two-dimensional (2-D) aperture to perform the imaging process that coherently integrates data from this 2-D aperture. In this case, without compensation, the phase and shape distortions in the original radar signatures would result in poorly focused SAR imagery. Figure 11a (left) shows a SAR image with data from the forward-looking ARL SIRE radar. The SAR image

covers an area of 25 m in cross-range direction and 64 m in down-range (or forward) direction. In this run, the radar moves very slow at an average speed of 1 m/sec. All the signal processing steps are applied to the data except this forward motion compensation processing. Figure 11b (right) shows the same SAR image (plotted with the same dynamic range) with all the signal-processing steps (that include the forward motion compensation processing) applied to the radar data. It is obvious that without the forward motion processing, the targets in figure 11a do not preserve the original shapes and significantly suffer the loss of their radar cross-sectional values. Also note that the details of the clutter strip on the right side of the SAR image are lost in figure 11a. Figure 12 shows the image chips of four in-scene targets with (right column) and without (left column) the forward motion processing. The forward motion processing improves the peak's levels of the targets from 5 dB to 13 dB in this case. More importantly, without processing, the shape distortions will lead to the wrong frequency contents. For a typical target detection system (*11*), the textures and frequency contents of the targets play important roles in the discrimination of targets against other confuser classes.
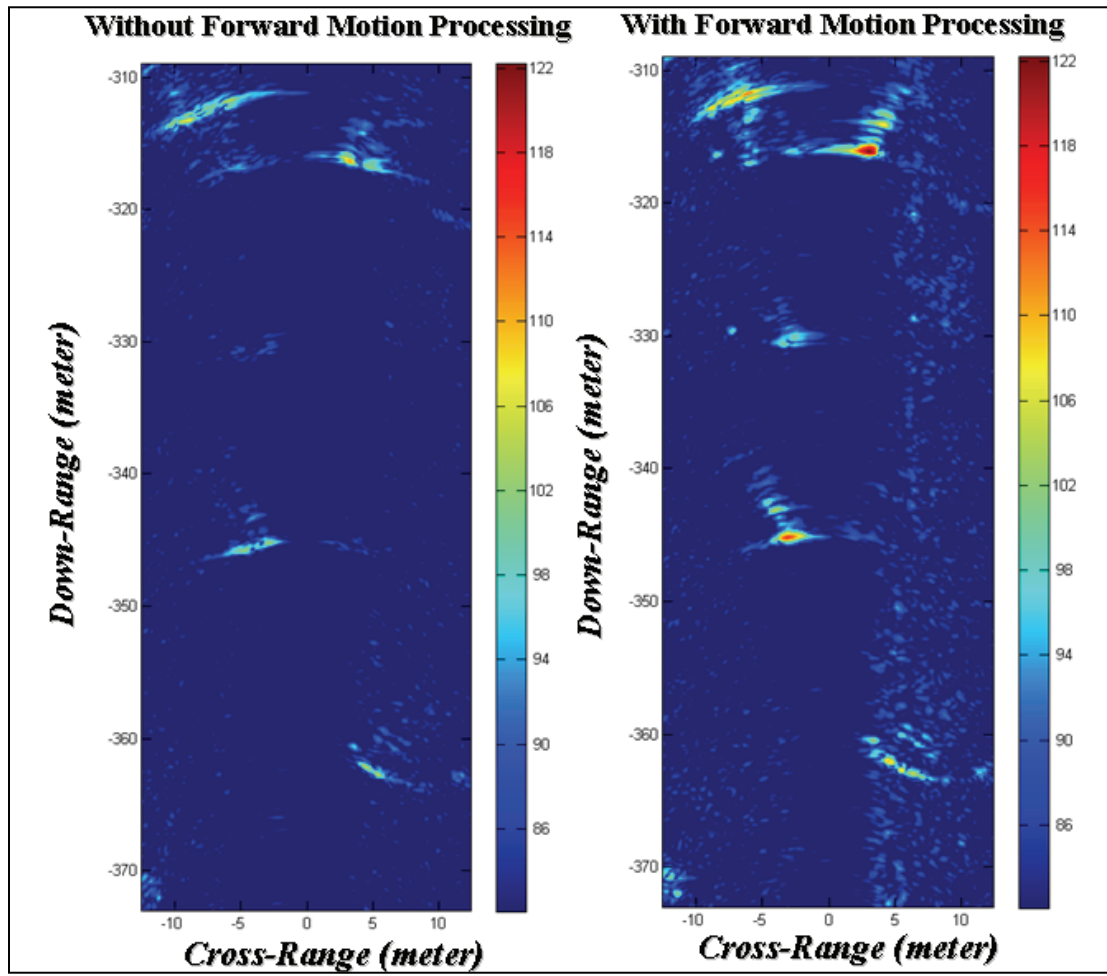
Figure 11. SAR image using data from the forward-looking ARL SIRE radar. (The SAR image on the left does not have the application of the forward motion-processing algorithm. The SAR image on the right shows the result after the forward motion-processing technique has been applied to the radar data.)
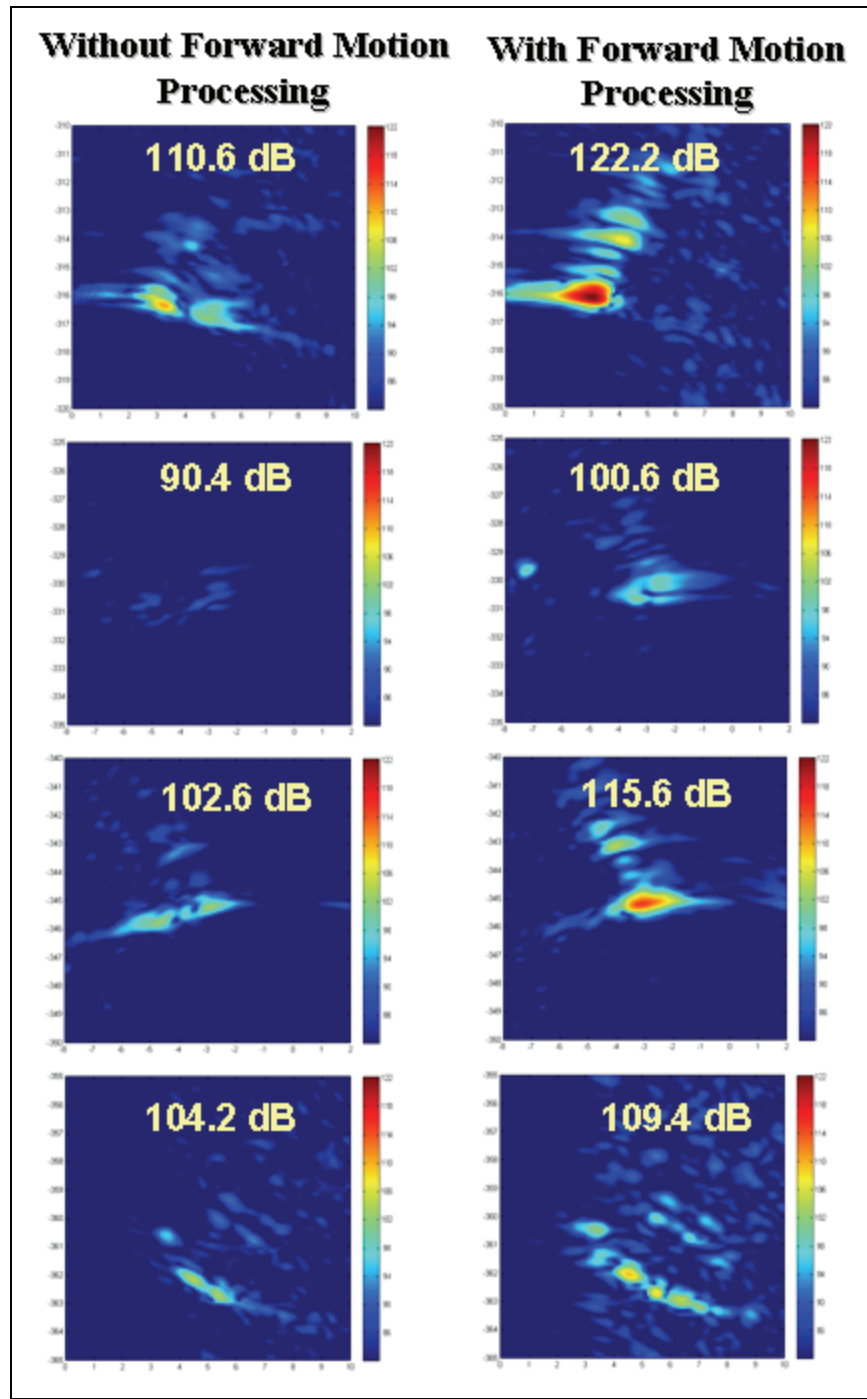
Figure 12. SAR image chips of targets before (left) and after (right) the processing
of the forward motion algorithm. (The forward motion processing improves
the peak's levels of the targets from 5 dB to 13 dB in this case.)

3. Summary

ARL has designed and developed the SIRE UWB SAR radar in support of the U.S. Army vision for increased mobility, survivability, and lethality. The radar is based on time-domain wideband impulses. For this radar, ARL designed and implemented a data acquisition technique called SIRE that allowed us to employ relatively slow ADC (40 MHz) to digitize wideband signals (>3000 MHz). However, the scheme assumed that the radar and targets are stationary during the data acquisition cycle when in reality, the target signatures did suffer the distortions in phase and shape because of the radar motion. The phase error would lead to significant loss in target radar cross-sectional values in resulting SAR imagery. The shape errors would destroy the frequency contents of the targets and thus the ability to discriminate targets from other confuser classes.

This report described a signal-processing method that we designed to recover the accuracy of the target signatures that were affected by the radar motion. We applied the signal-processing method to simulated data and measured data from ARL SIRE radar. With the simulated data, we showed the perfect reconstruction using this method. With the measured radar data, we demonstrated significant improvement in the resulting SAR image. The radar cross section of targets improved from 5 dB to 13 dB. The correct shapes of target signatures are preserved.

4. References

1. Nguyen, Lam; Wong, David; Ressler, Marc; Koenig, Francois; Stanton, Brian; Smith, Gregory; Sichina, Jeffrey; Kappra, Karl. Obstacle Avoidance and Concealed Target Detection Using the Army Research Lab Ultra-Wideband Synchronous Impulse Reconstruction (UWB SIRE) Forward Imaging Radar. *Proceedings of SPIE, Detection and Remediation Technologies for Mines and Minelike Targets XII*, Vol. 6553, April 2007.

2. Ressler, Marc; Nguyen, Lam; Koenig, Francois; Wong, David; Smith, Gregory. The Army Research Laboratory (ARL) Synchronous Impulse Reconstruction (SIRE) Forward-Looking Radar. *Proceedings of SPIE, Unmanned Systems Technology IX*, Vol. 6561, May 2007.

3. Ressler, Marc; Nguyen, Lam; Koenig, Francois; Smith, Gregory. Synchronous Impulse Reconstruction (SIRE) Radar Sensor for Autonomous Navigation. *Army Science Conference*, November 2006.

4. Real-Time Versus Equivalent-Time Sampling, Tektronix, http://www.tek.com/Measurement/ cgi-bin/framed.pl?Document=/Measurement/App_Notes/RTvET/ap-RTvET.html&FrameSet=oscilloscopes

5. RAMAC/GPR Borehole radar, Mala Geoscience USA, Inc., www.malags.com

6. Theory and Application of Digital Signal Processing by Lawrence R. Rabiner, Bernard Gold, Prentice Hall, Inc1975.

7. McCorkle, John; Nguyen, Lam. *Focusing of Dispersive Targets Using Synthetic Aperture Radar*; ARL-TR-304; U.S. Army Research Laboratory: Adelphi, MD, August 1994.

8. Nguyen, Lam H.; Kapoor, Ravinder; Sichina, Jeffrey. Detection algorithms for ultrawideband foliage-penetration radar. *Proceedings of SPIE*, Volume 3066, Radar Sensor Technology II, June 1997, pp. 165–176

9. Nguyen, Lam H.; Kappra, Karl A.; Wong, David C.; Kapoor, Ravinder; Sichina, Jeffrey. Mine field detection algorithm utilizing data from an ultrawideband wide-area surveillance radar. *Proceedings of SPIE -- Volume 3392, Detection and Remediation Technologies for Mines and Minelike Targets III*, September 1998, pp. 627–643

10. Nguyen, Lam H.; Wong, David C.; Smith, Gregory; Ressler, Marc A. Forward imaging robotic vehicle mission using an ultra-wideband synthetic aperture radar. *Proceedings of SPIE, Volume 4715, Unmanned Ground Vehicle Technology IV*, July 2002, pp. 355–364

11. Nguyen, Lam; Kappra, Karl; Wong, David; Kapoor, Ravinder; Sichina, Jeffrey. A Mine Field Detection Algorithm Utilizing Data from an Ultra-Wideband Wide-Area Surveillance Radar. *SPIE Conference on Detection and Remediation Technologies for Mines and Minelike Targets Ill*, SPIE Vol. 3392, 1998

Distribution List

No. of Copies	Organization
1	ADMNSTR DEFNS TECHL INFO CTR ATTN DTIC OCP (ELECTRONIC COPY) 8725 JOHN J KINGMAN RD STE 0944 FT BELVOIR VA 22060-6218
1	DARPA ATTN IXO S WELBY 3701 N FAIRFAX DR ARLINGTON VA 22203-1714
1	OFC OF THE SECY OF DEFNS ATTN ODDRE (R&AT) THE PENTAGON WASHINGTON DC 20301-3080
1	US ARMY RSRCH DEV AND ENGRG CMND ARMAMENT RSRCH DEV AND ENGRG CTR ARMAMENT ENGRG AND TECHNLGY CTR ATTN AMSRD AAR AEF T J MATTS BLDG 305 ABERDEEN PROVING GROUND MD 21005-5001
1	US ARMY TRADOC BATTLE LAB INTEGRATION & TECHL DIRCTRT ATTN ATCD B 10 WHISTLER LANE FT MONROE VA 23651-5850
1	PM TIMS, PROFILER (MMS-P) AN/TMQ-52 ATTN B GRIFFIES BUILDING 563 FT MONMOUTH NJ 07703
1	US ARMY INFO SYS ENGRG CMND ATTN AMSEL IE TD F JENIA FT HUACHUCA AZ 85613-5300

No. of Copies	Organization
1	COMMANDER US ARMY RDECOM ATTN AMSRD AMR W C MCCORKLE 5400 FOWLER RD REDSTONE ARSENAL AL 35898-5000
1	US ARMY RSRCH LAB ATTN AMSRD ARL CI OK TP TECHL LIB T LANDFRIED BLDG 4600 ABERDEEN PROVING GROUND MD 21005-5066
1	US GOVERNMENT PRINT OFF DEPOSITORY RECEIVING SECTION ATTN MAIL STOP IDAD J TATE 732 NORTH CAPITOL ST NW WASHINGTON DC 20402
1	DIRECTOR US ARMY RSRCH LAB ATTN AMSRD ARL RO EV W D BACH PO BOX 12211 RESEARCH TRIANGLE PARK NC 27709
18	US ARMY RSRCH LAB ATTN AMSRD ARL CI OK T TECHL PUB ATTN AMSRD ARL CI OK TL TECHL LIB ATTN AMSRD ARL SE RU L NGUYEN (5 COPIES) ATTN IMNE ALC IMS MAIL & RECORDS MGMT ATTN AMSRD ARL-SE-RU M RESSLER ATTN AMSRD ARL SE RU F KOENIG ATTN AMSRD ARL SE RU D WONG ATTN AMSRD ARL SE RU C TRAN ATTN AMSRD ARL SE RU G SMITH ATTN AMSRD ARL SE RU G KIROSE ATTN AMSRD ARL SE RU K RANNEY ATTN AMSRD ARL SE RU K KAPPRA ATTN AMSRD ARL SE RU J SICHINA ATTN AMSRD ARL SE RU A SULLIVAN ADELPHI MD 20783-1197